

MIT Open Access Articles

A Smart Online Over-Voltage Monitoring and Identification System

The MIT Faculty has made this article openly available. **Please share** how this access benefits you. Your story matters.

Citation: Wang, Jing et al. "A Smart Online Over-Voltage Monitoring and Identification System." *Energies* 4 (2011): 599-615. © 2011 by the authors

As Published: <http://dx.doi.org/10.3390/en4040599>

Publisher: Molecular Diversity Preservation International

Persistent URL: <http://hdl.handle.net/1721.1/66178>

Version: Author's final manuscript: final author's manuscript post peer review, without publisher's formatting or copy editing

Terms of use: Creative Commons Attribution 3.0



Article

A Smart Online Over-Voltage Monitoring and Identification System

Jing Wang ¹, Qing Yang ^{1,2,*}, Wenxia Sima ¹, Tao Yuan ¹ and Markus Zahn ²

¹ State Key Laboratory of Power Transmission Equipment & System Security and New Technology, Chongqing University, Chongqing, China; E-Mails: bjjdwj@cqu.edu.cn (J.W.); cqsmwx@cqu.edu.cn (W.S.); yuantao_cq@cqu.edu.cn (T.Y.)

² Research Laboratory of Electronics, Laboratory for Electromagnetic and Electronic Systems, High Voltage Research Laboratory, Department of Electrical Engineering and Computer Science, Massachusetts Institute of Technology, Cambridge, MA 02139, USA; E-Mail: zahn@mit.edu

* Author to whom correspondence should be addressed; E-Mail: yangqing@cqu.edu.cn; Tel.: +86-23-65112738; Fax: +86-23-65112739.

Received: 24 February 2011; in revised form: 6 April 2011 / Accepted: 15 April 2011 /

Published: 18 April 2011

Abstract: This paper proposes a complete and effective smart over-voltage monitoring and identification system. In recent years, smart grids are of the greatest interest in power system research. One of the main features of smart grid is their self-healing, which can continuously carry out online self-evaluation, discover existing faults, and correct them immediately. The over-voltage smart monitoring-identification-suppression systems play a key role in the construction of self-healing grids. In this paper, eight kinds of common over-voltage are discussed and analyzed. The S-transform algorithm is used to extract features of over-voltage. Aiming at the main features of each kind of over-voltage, six different characteristic quantities are proposed. A well designed fuzzy expert system and a support vector machine are employed as the classifiers to build a two-step identification model. The accuracy of the identification system is verified by field records. Results show that this system is feasible and promising for real applications.

Keywords: smart grid; over-voltage; identification; S-transform; fuzzy expert system

1. Introduction

Recently, with the increasing demand for electric power and the rising complexity of power networks, smart grids with self-healing characteristics are of the greatest interest in power system research [1]. Self-healing grids can continuously carry out online self-evaluation to predict the problems the grid may encounter, discover existing or imminent problems, and immediately take control or implement corrective measures to ensure the reliability, safety, power quality and efficiency of the grid [2]. To form a complete smart monitoring and suppression system integrated advanced monitoring, control and protection technology are required so as to provide real-time monitoring, online identification and smart restrictions for the potential over-voltage during the operation of the power system, which will be very important for the construction of the smart grid.

Over-voltage is the direct reflection of power system faults. Research and development of over-voltage online monitoring-identification-suppression systems has great significance to the self-healing grid. At present, over-voltage monitoring systems are usually designed and developed based on a potential transformer system and the resistor or capacitor voltage-dividing system. These systems are mostly used in the distribution grids, and are hardly used in 110 kV system monitoring or even for higher power levels, because of a series of problems arising after working for long durations such as the reliability and heating problem, and especially safety issues for personal and measuring equipment. Therefore, the development of new sensors is urgently needed. The sensor introduced in this paper has the advantages of small size, high levels of insulation, good behavior in steady state and transient response. It is suitable for over-voltage online monitoring and recording.

The over-voltage identification system plays a transitional role in the over-voltage smart suppression system. It can classify and identify the over-voltage signals coming from the online monitoring and recording equipment, and then start the appropriate suppression operations based on the identification results. The accuracy rate of classification and identification will directly influence the effectiveness of the over-voltage suppression.

There are two key factors in the over-voltage identification research. The first factor is the requirement of adequate field over-voltage records. Many over-voltage identification researches are based on simulated signals [3,4], but the field conditions of a power system are very complex, and the nonlinear parameters of the power system can not be represented precisely in the simulations or theoretically. Therefore, those identification systems developed based on simulation signals are not feasible for real applications. The second factor is finding the appropriate algorithms and methods, including feature extraction algorithms and classifiers, which directly affect the identification rate.

In this paper, a smart over-voltage monitoring system which was developed by Chongqing University and used for online over-voltage monitoring is introduced. Large amounts of field over-voltage records have been recorded and stored, thus meeting the requirement of adequate field over-voltage records for over-voltage identification research. This kind of over-voltage monitoring system is the basis for the smart control of the over-voltage in power systems.

Identification systems always contain two main parts: feature extraction and classifier. Short time Fourier transform (STFT) and wavelet transform (WT) are the most widely used time-frequency analysis algorithms in voltage signal analysis and feature extraction [5–7]. The ability of time domain analysis of STFT is based on a fixed window, so it can not be used to successfully analyze nonlinear

signals such as over-voltage signals. WT is a well known multi-resolution analysis algorithm due to its adaptable scaling properties. It has the ability to analyze the signals in both the frequency and time domains. S-transform (ST) [8] is an advanced time-frequency algorithm that combines the advantages of STFT and WT [9,10] and has been widely used in analysis and identification of power signals [3,9–11]. ST can be regarded as a scalable window STFT or a deformation of a continuous wavelet transform. Therefore, ST shows different performance for different frequency components because of the scalable window. For the high-frequency components of the signal, the window width of ST is narrow, thus time resolution is good. For the low-frequency components, ST has high frequency resolution, which make it a good over-voltage feature extraction algorithm candidate.

Different kinds of over-voltage have different features. Some features can be represented by the characteristic quantities' value, such as the amplitude of the 50 Hz component. The higher the value, the more possible the type of over-voltage is fundamental ferroresonance or single phase-to-ground, although some features have no close relationship with this value. For example, the sub-frequency ferroresonance feature is represented by its 16.6 Hz or 25 Hz harmonic. If this harmonic can be observed, the over-voltage must be a sub-frequency ferroresonance, otherwise it is not. This is a kind of 'IF or NOT' judging approach, and has no relationship with the frequency value itself. Therefore, in this paper, compared with some widely used classifiers, such as artificial neural networks (ANN) and support vector machine (SVM), the fuzzy expert system (FES) is employed as the main classifier. FES has been successfully used in many areas, such as speech recognition [12], power quality disturbances classification [13] and power system fault diagnosis [14].

2. Over-Voltage Monitoring System

2.1. Over-Voltage Sensor

The development of an over-voltage sensor is a key part of any online monitoring system. At present, the over-voltage monitoring devices used in the distribution network, are mostly based on the potential transformer system and resistor or capacitor voltage-dividing systems. If the voltage-dividing system is connected in parallel to the grids for a long time, the heat problem will become more serious. Furthermore, the high arm and the low arm of the voltage-dividing system are not isolated from each other, which may threaten the monitoring devices and human safety.

In this paper, a special voltage sensor is designed and installed to form the bushing voltage-divider system to collect voltage signals from the tap of the capacitance bushing (Figure 1), so as to realize real-time collection of grid over-voltage signals.

The voltage sensor is installed at the transformer bushing top. The circuit diagram of the voltage sensor is shown in Figure 2, where C_S is the divider capacitance, R_S is the divider resistance, R_P is a matching resistance and P_S is a protective unit. The voltage-dividing unit is composed of a dividing capacitance and dividing resistance, respectively constituting the high-frequency response and low-frequency response closed circuit. In order to reduce the magnetic coupling between the elements of the voltage-dividing unit and the output circuit, as well as to minimize the influence of residual inductance on the response characteristics of the sensor, the sensor structure adopts a coaxial cylinder structure. The matched resistance is connected to the signal transmission cable interface through the

center of the sensor. The resistance and capacitance voltage-dividing elements are connected in parallel and arranged symmetrically around the circumference toward the center. The outermost shell of the whole sensor is the metal shell. It is designed to realize electromagnetic shielding for core components through the grounded metal shell.

Figure 1. Installation diagram of transformer bushing top.

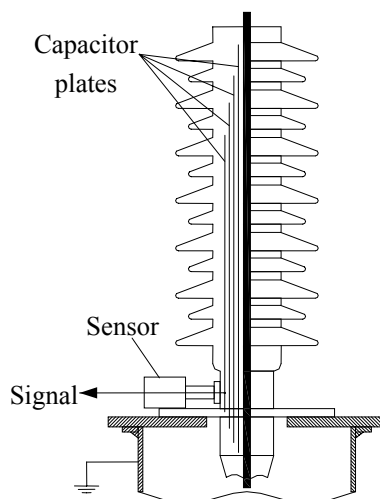
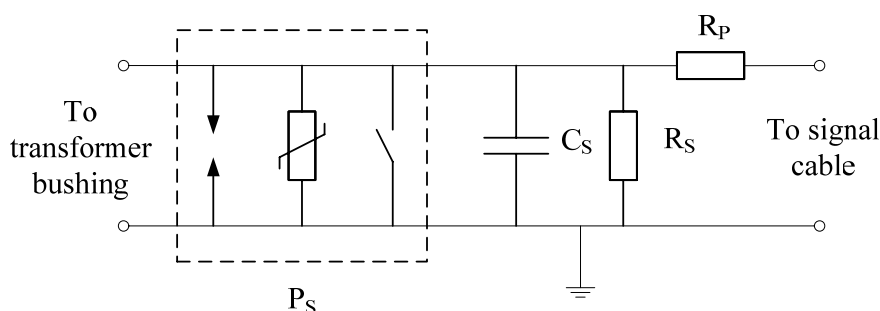


Figure 2. Simulation model of voltage sensor that mounted at the tap of transformer bushing.



The voltage sensor is installed at the measuring tap of the transformer capacitance bushing. When over-voltage signals initiate, the sensor will first transform the high-voltage over-voltage signals into corresponding low-voltage signals and then send them to the signal processing front-end circuit through the coaxial cable. After the output signals of the sensor are necessarily conditioned by the front-end circuit, the output signals will be sent to the data acquisition card for collection. The whole over-voltage data acquisition system is mainly composed of a signal conditioning circuit, trigger circuit, protection unit control circuit, data acquisition card and corresponding acquisition software.

2.2. Online Monitoring System

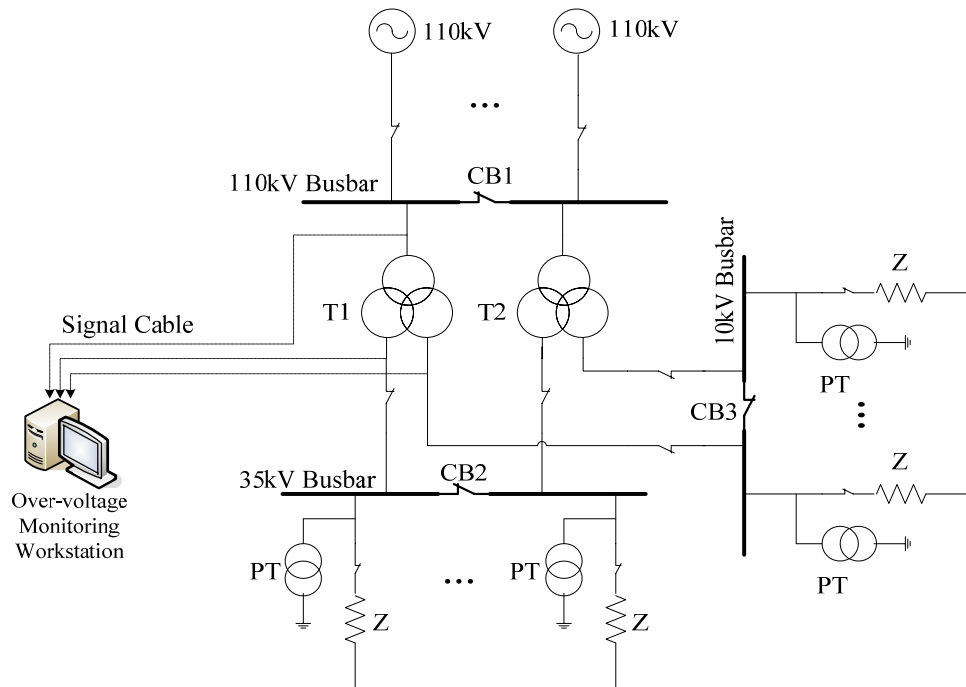
The signal conditioning circuit is composed of a two stage amplifier: the first stage amplifier is a voltage follower and the second stage amplifier is a lowpass filter. The output signals are transmitted to the data acquisition card through the signal cable. The amplifier uses an AD817 high-speed and low-power-consumption operational amplifier produced by Analog Devices Corp. The data acquisition

card of this device employs a PCI-9812 data acquisition card, which is based on a 32-bit PCI bus, 12-bit resolution, on chip 32 k bytes FIFO buffer and a maximum sampling frequency of 20 MHz.

With the maximum sampling frequency of 5 MHz on the whole, this online monitoring data acquisition system has adopted a pre-trigger principle and frequency conversion sampling principle. After it is started, the acquisition system will start to sample as per the sampling frequency of 5 MHz and start the counter. When the counter records a certain length, the AD sampling and address generator clock will turn into the stated frequency of 200 kHz till the completion of the whole data acquisition course. This sampling mode has taken data storage cost into account. It has adopted a high-accuracy sampling rate to record the over-voltage peak characteristics as accurately as possible and has adopted a comparatively low sampling rate to record the comparatively long-term wave form as long as possible so as to meet the internal over-voltage demand of the monitoring power system and the atmospheric over-voltage demand at the same time.

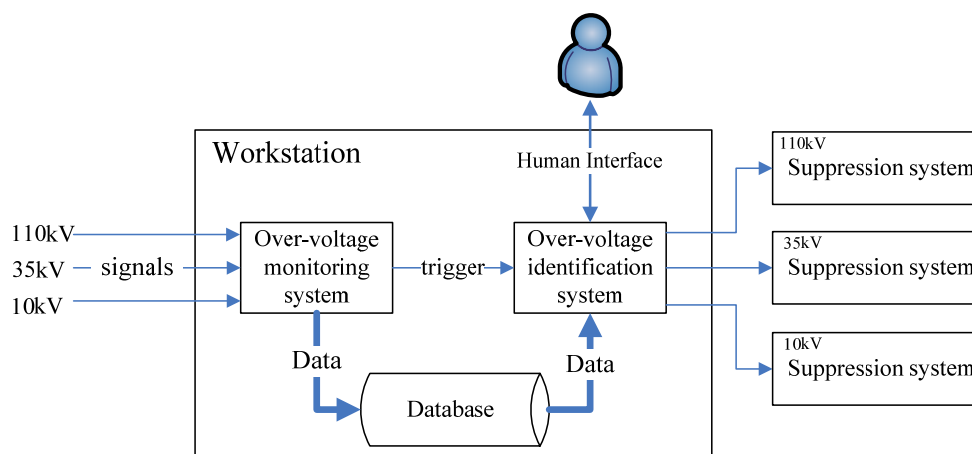
The intelligent monitoring systems have been put into operation in Chongqing. The wiring diagram of the monitoring system in the substation is shown as Figure 3. This substation contains three different voltage levels. There are six feeders on the 35 kV bus bar, and 5 feeders on the 10 kV bus bar. T1 and T2 is the main transformer, and the capacity of each is 31.5 MVA. CB1–CB3 are current breakers. The voltages of 110 kV, 35 kV and 10 kV are monitored through three sensors. The sensors are connected to the monitoring workstation through the signal cable.

Figure 3. Wiring diagram of monitoring system in the substation.



3. Over-Voltage Identification System

The software of monitoring system and identification system are installed in the same workstation. Once the amplitude of voltage exceeds the threshold, the monitoring system records the waveforms of voltage and stores them in the database in the form of discrete data. Then the over-voltage identification system is triggered to classify and identify this record. The workflow is described in Figure 4.

Figure 4. Workflow of over-voltage monitoring-identification-suppression system.

The monitoring system, identification system and the database are independent from each other. This working scheme has a high stability. If a fault occurs in one part, it does not affect the others. In particular, it can reduce the risk of data corruption greatly. Meanwhile the upgrade of software is more convenient.

This over-voltage online identification system includes the following key features:

- Online over-voltage identification.
- Trigger the suppression system at the next level, and alert the operator through human interface.
- Searching and analysis of past over-voltages from the database.
- Statistics of appearance frequency for different kinds of over-voltage in different power grids.

In whole identification system research, the over-voltage identification method is the most important and difficult part. This over-voltage identification system can serve for three different power grids: 110 kV grounded neutral network, 35 kV and 10 kV isolated neutral networks. The over-voltages will show some difference on its type or features in different neutral grounding modes and different power levels. For example, the arc grounding fault only occurs in the isolated neutral networks, and the amplitude of switching over-voltage is higher in the 110 kV networks. Even so, the methods and algorithms of over-voltage identification for different power levels are still similar to each other. In this paper, the 10 kV identification system is discussed and used as an example.

4. S-Transform and Feature Extraction for Over-Voltage Records

Over-voltage signals form a nonlinear time series. Some over-voltage's features are represented in high frequency transient oscillations, such as due to lightning. Some over-voltage's features are represented at their harmonics, such as ferroresonance. In order to reflect the features of different kinds of over-voltages, S-transform is employed to analyze and extract the features of voltage signals.

4.1. S-Transform

The ST is a reversible local time-frequency analysis, proposed by Stockwell in 1996 [8]. Given a time domain signals $h(t)$, the S-transform can be described as follows:

$$S(\tau, f) = \int_{-\infty}^{\infty} h(t) w(\tau - t, f) e^{-j2\pi ft} dt \tag{1}$$

where $w(\tau - t, f)$ is the Gaussian window:

$$w(\tau - t, f) = \frac{f}{\sqrt{2\pi}} e^{(-f^2(\tau-t)^2/2)} \tag{2}$$

The original signal $h(t)$ can be obtained from $S(\tau, f)$ through an inverse S-transformation:

$$h(t) = \int_{-\infty}^{\infty} \left\{ \int_{-\infty}^{\infty} S(\tau, f) d\tau \right\} e^{j2\pi ft} df \tag{3}$$

The ST spectrum $S(\tau, f)$ also can be obtained from the Fourier transform $h(t)$ of the original signal $h(t)$

$$S(\tau, f) = \int_{-\infty}^{\infty} H(\alpha + f) e^{(-2\pi^2\alpha^2/f^2)} e^{-j2\pi ft} d\alpha \tag{4}$$

where $h[kT]$ ($k = 0, 1, \dots, N - 1$) is the discrete form of the original signal $h(t)$, where T is the sampling period. Then the discrete Fourier transform of $h[kT]$ can expressed as:

$$H\left[\frac{n}{NT}\right] = \frac{1}{N} \sum_{k=1}^{N-1} h[kT] e^{-j2\pi nk/N} \tag{5}$$

where $n = 0, 1, \dots, N - 1$.

Let $f \rightarrow n/NT$ and $\tau \rightarrow jT$ in Equation (4), then the discrete version of ST can be described as:

$$\begin{cases} S\left[kT, \frac{n}{NT}\right] = \sum_{m=0}^{N-1} H\left[\frac{m+n}{NT}\right] e^{-\frac{2\pi^2 m^2}{n^2}} e^{\frac{j2\pi mk}{N}} & n \neq 0 \\ S[jT, 0] = \frac{1}{N} \sum_{m=0}^{N-1} h\left[\frac{m}{NT}\right] & n = 0 \end{cases} \tag{6}$$

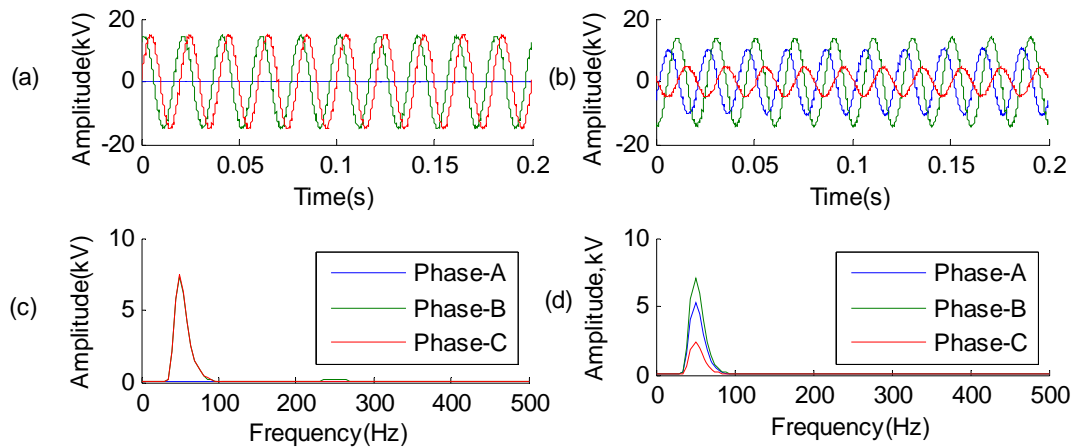
Therefore ST can be calculated rapidly by employing the FFT. The result of ST is an S-matrix, with rows pertaining to frequency and columns pertaining to time. Both phase and amplitude information of signals can be presented by ST.

4.2. Feature of Over-Voltage

The types of over-voltage studied in this paper include: single phase-to-ground, high frequency ferroresonance, fundamental ferroresonance, sub-frequency ferroresonance, arc grounding, capacitor switching, line switching and lightning. The features of each kind of over-voltage are discussed below.

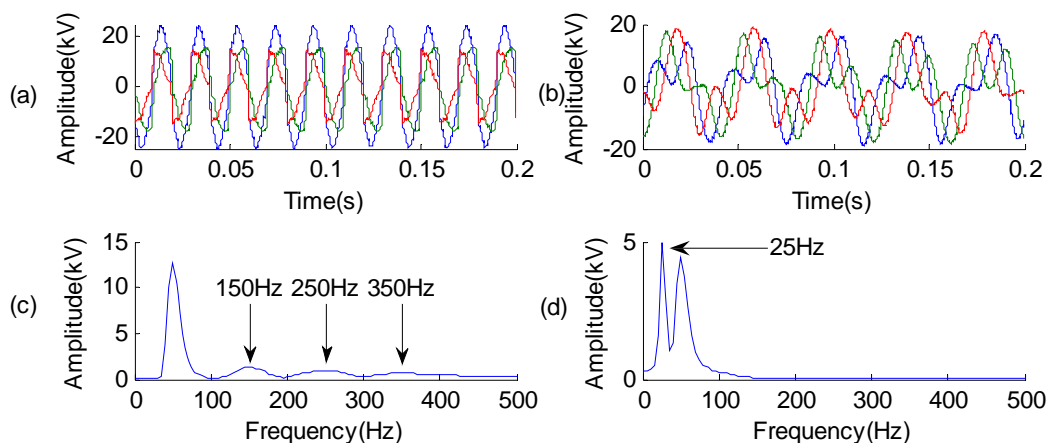
- (1) When a single phase-to-ground occurs, the voltage in the fault phase drops to zero, and the other two phase voltages increase. Typical waveforms are shown in Figure 5a.
- (2) When a fundamental ferroresonance takes place, a power frequency over-voltage is shown in the power system, the amplitude in three phases can be expressed by three cases:
 - (i) The voltage in one phase drops but not equal to zero, and the other two increase (Figure 5b).
 - (ii) The voltage in two phases drop and the other one increase.
 - (iii) The voltages in three phases all increase.

Figure 5. (a) Single phase-to-ground voltage; (b) Fundamental ferroresonance; (c) Mean amplitude curve of single phase-to-ground voltage; (d) Mean amplitude curve of fundamental ferroresonance.



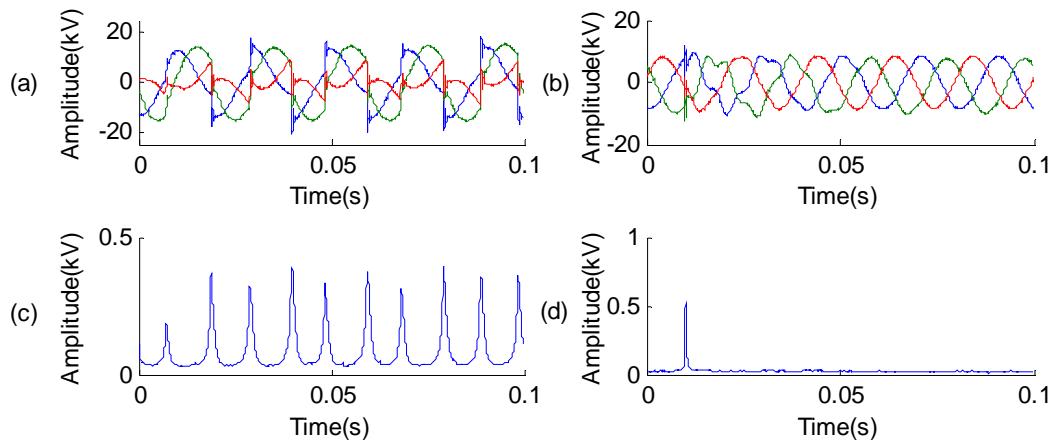
- (3) If a high frequency ferroresonance occurs, the voltage in the three phases contain 150 Hz, 250 Hz, 350 Hz harmonics (3, 5, 7 times of 50 Hz power frequency). A typical waveform is shown in Figure 6a.
- (4) If a sub-frequency ferroresonance occurs, the voltage signals in the three phases contain 25 Hz or 16.6 Hz harmonics (1/2, 1/3 of power frequency). A typical waveform is shown in Figure 6b.

Figure 6. (a) High frequency ferroresonance; (b) Sub-frequency ferroresonance; (c) Mean amplitude curve of high frequency ferroresonance; (d) Mean amplitude curve of sub-frequency ferroresonance.



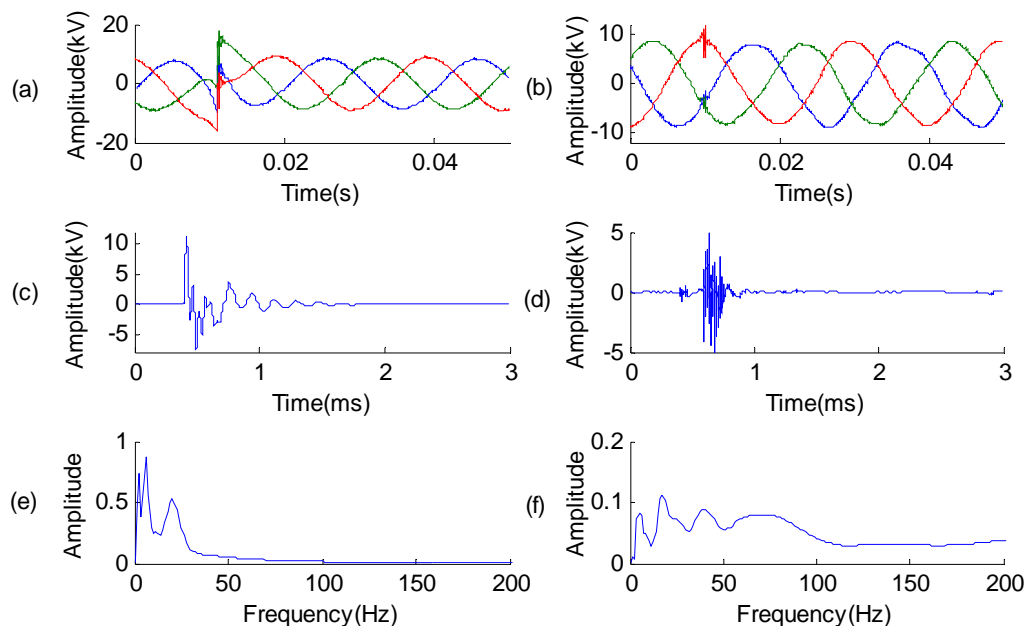
- (5) When the arc ground fault takes place in the system, the arc at the fault point will extinguish and rekindle repeatedly. It is presented as repeated high-frequency oscillations on the waveform. A typical waveform is shown in Figure 7a.
- (6) When a capacitor switching occurs, the power voltage component does not change too much, and the high frequency oscillation is highly similar with the line switching. A damping harmonic with the frequency around 200 Hz will occur at the switching moment, which is the major feature of a switch capacitor. A typical waveform is shown in Figure 7b.

Figure 7. (a) Arc grounding; (b) Capacitor switching; (c) Mean amplitude curve of arc grounding; (d) Mean amplitude curve of capacitor switching.



(7) The main feature of lightning and line switching over-voltage is shown in their high frequency oscillation. General, the power frequency component will not change too much after these two over-voltages take place. Typical waveforms of lightning and line switching are shown in Figures 8a,b.

Figure 8. (a) Lightning; (b) Line switching; (c) Transient oscillation of lightning; (d) Transient oscillation of line switching; (e) Mean amplitude curve of lightning; (f) Mean amplitude curve of line switching.



Benefiting from the unique sampling model of over-voltage monitoring devices in this paper, the initial part of the over-voltage waveform is sampled at 5 MHz. Therefore the high frequency oscillation can be represented in detail through the discrete data (Figures 8c,d). It is clear that the transient oscillation's frequency of line switching is higher than lightning. Figures 8e, f are the mean amplitude curves of the transient oscillation of lightning and line switching (Figures 8c,d).

4.3. Feature Extraction

In the signals identification research, features extraction is very important, and characteristic quantities must represent the most typical features of over-voltage precisely. Based on the above analysis, six kinds of characteristic quantities are extracted and employed in the identification system.

It should be noted that, except the 3rd characteristic quantity, the other characteristic quantities are all extracted from the phase with the largest root mean square (RMS).

- (1) The proportion of power frequency component (50 Hz) in the whole frequency spectrum.

Define:

$$AvsF(f) = \sum_{k=1}^N \left| S(kT, \frac{n}{NT}) \right| \quad (7)$$

then:

$$CQ1 = \frac{\sum_{f=40}^{60} AvsF(f)}{\sum_f AvsF(f)} \quad (8)$$

This characteristic quantity is used to judge if there are large harmonics existing in the signal. For example, fundamental ferroresonance over-voltage only contains a 50 Hz component, line switching over-voltage contains high frequency oscillations, but the duration of oscillations is very short, therefore the 50 Hz component should occupy a large proportion for these two, and there are no existing large harmonics.

- (2) The average amplitude of the power frequency component (50 Hz):

$$CQ2 = \frac{\sum_{k=1}^N |S(kT, 50)|}{N \times V_{nml}} \quad (9)$$

where V_{nml} is the normal power frequency component's amplitude; in this paper $V_{nml} = 10.5/\sqrt{6} \approx 4.2866$.

This characteristic quantity is used to divide the single phase-to-ground and fundamental ferroresonance from others.

- (3) The smallest RMS of the voltages in the three phases:

$$CQ3 = RMS(\min(U_A, U_B, U_C)) \quad (10)$$

where $CQ3$ is close to zero for a single phase-to-ground, and is small but not equal to zero for fundamental ferroresonance.

- (4) In the amplitude-time spectrum, the peak value of high frequency parts, which is used to determine whether a high frequency oscillation exists:

$$AvsT_{500}(kT) = \sum_{n=500 \times NT} \left| S(kT, \frac{n}{NT}) \right| \quad k = \{1, 2, \dots, N\} \quad (11)$$

$$CQ4 = \frac{\max\{AvsT_{500}(kT)\}}{\sum_{k=1}^N AvsT_{500}(kT)} \times N \quad (12)$$

(5) Calculate the amplitude-frequency spectrum in the period of 0.005 s–0.04 s. $CQ5$ is the frequency of the highest peak except for the 50 Hz peak. For example, if the over-voltage is sub-frequency ferroresonance (Figure 6b) then $CQ5$ is 25. If the over-voltage is high-frequency ferroresonance (Figure 6a) then $CQ5$ is 150. The reason why the time period is between 0.005 s and 0.04 s, is because the duration of capacitor switching over-voltage's 200 Hz harmonic is short, and the amplitude is relatively low. If this characteristic quantity is obtained from the whole time domain, then the harmonic of capacitor switching over-voltage will not be obvious enough, and confused with the other frequency components. The characteristic quantities of the over-voltages shown in Figures 5–8 are listed in Table 1.

It can be seen from the Table 1 that the line switching and lightning over-voltage are highly similarity in $CQ1$ – $CQ5$. In order to classify these two kinds of over-voltage, a new characteristic quantity is extracted from their transient oscillations.

Table 1. The first to fifth characteristic quantities.

Type	$CQ1$	$CQ2$	$CQ3$	$CQ4$	$CQ5$
Capacitor switching	0.6192	1.0220	0.9820	24.3205	185
Arc grounding	0.3977	1.8304	0.5030	6.5734	190
High frequency ferroresonance	0.4007	2.9556	1.6254	2.3694	150
Fundamental ferroresonance	0.6145	1.6446	0.7443	2.0455	0
Sub-frequency ferroresonance	0.4277	1.0160	1.5705	2.5649	25
Single phase-to-ground	0.7110	1.7279	0.0125	2.3310	0
Line switching	0.6757	1.0092	0.9891	15.7937	0
Lightning	0.6280	1.0447	0.9654	43.1868	0

(6) $CQ6$ is an array containing five elements. This characteristic quantity is obtained from the mean amplitude curve of transient oscillations (Figure 8e,f), by dividing the frequency domain into five parts: from 500 Hz to 10 kHz, 10 kHz to 25 kHz, 25 kHz to 100 kHz, 100 kHz to 200 kHz, and 200 kHz to max frequency. The characteristic quantities of the transient oscillations shown in Figure 8e,f are listed in Table 2.

Table 2. The sixth characteristic quantity.

Type	$CQ6$				
Line switching	0.0098	0.0134	0.0303	0.0250	0.9215
Lightning	0.3266	0.3437	0.2271	0.0290	0.0739

5. Over-Voltage Identification System

The advantage of Fuzzy Expert Systems is that researchers can assign certain rules to classification processes based on experience or theory. The black-box training mode of artificial neural networks and support vector machine is hard to be controlled. A controllable classifier is important for some specific features, such as the fifth characteristic quantities.

5.1. Fuzzy Expert System

A Fuzzy Expert System contains two major parts: fuzzy sets and a fuzzy rule base [15]. The concept of fuzzy sets was proposed by L.A. Zadeh in 1965 [16]. Given a fuzzy set A, let $x \in U$ be the elements, a membership function (MF) $\mu_A(x)$ presents how much x belongs to A, expressed as:

$$A = \{(x, \mu_A(x)), x \in U\} \tag{13}$$

The fuzzy rule base is the “IF-Then” constructions, which can be described as:

If x_1 is A_1 and x_2 is $A_2 \dots x_n$ is A_n then y is B

where $A_i (i = 1, 2, \dots, n)$ and B are linguistic values. There are many mature function expressions available for forming the membership function, such as triangular MF, trapezoidal MF, generalized bell MF and Gaussian MF. In this paper, so the distribution of characteristic quantity’s values are more closer to a normal distribution, so the Gaussian MF (normal distribution function) is employed as the membership function:

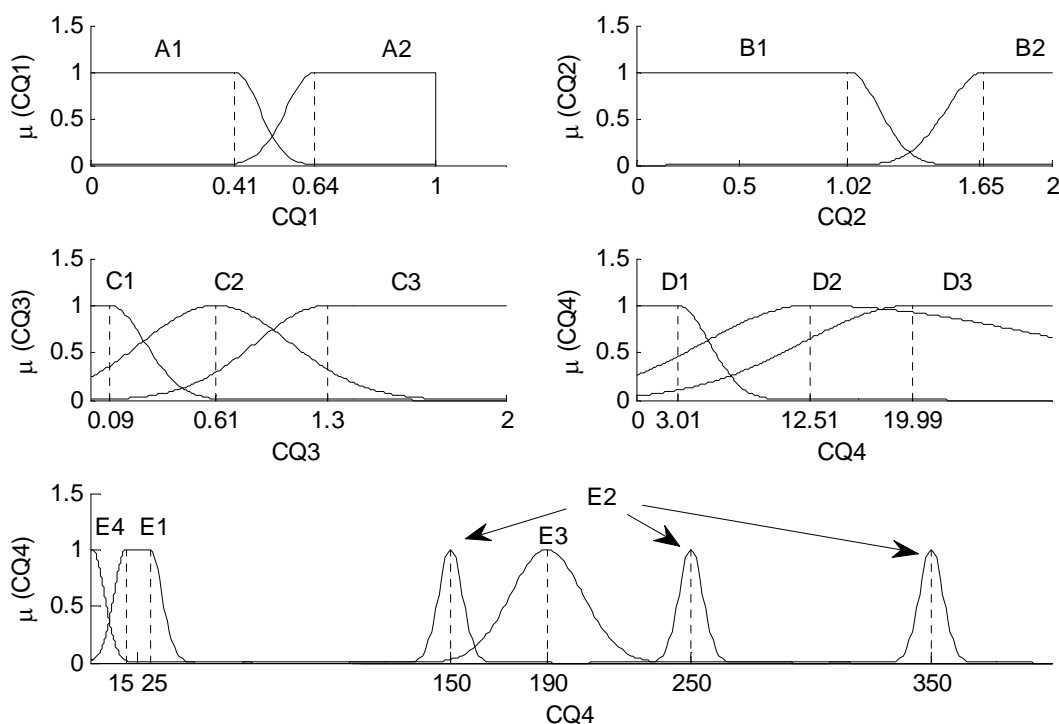
$$\mu_{A_i}(x_i) = e^{-\frac{(x_i - c)^2}{2\sigma^2}} \tag{14}$$

where c is the mean value and σ is the standard deviation, which determine the location and width of the membership functions.

5.2. Membership Function

The parameters of each membership function are obtained through the statistics of field records. Figure 9 shows the membership functions for characteristic quantities from CQ1 to CQ5.

Figure 9. Membership functions.



It should be clear that the center point c of $CQ5$ is not calculated from field records. It is defined by the over-voltage concept. For example, the main harmonic’s frequency of sub-frequency ferroresonance is 25 Hz or 16.6 Hz, and the sampling rate of ST in the frequency domain is decided by the original signal’s length ($f_s = 1/NT$, in this paper $f_s = 5$ Hz), and two center points are designated as 15 Hz and 25 Hz.

The standard deviation σ for each membership function is listed in Table 3. The membership function μ_{D2} has two standard deviation σ , because the distribution of $CQ4$ are uneven on two sides of the mean value c .

Table 3. Standard deviation σ for each membership function.

MF	σ	MF	σ
μ_{A1}	0.0709	μ_{D1}	2.3009
μ_{A2}	0.0797	μ_{D2}	7.6125/19.3283
μ_{B1}	0.1478	μ_{D3}	7.9675
μ_{B2}	0.1798	μ_{E1}	5
μ_{C1}	0.1721	μ_{E2}	5
μ_{C2}	0.3578	μ_{E3}	15
μ_{C3}	0.3405	μ_{E4}	5

5.3. Fuzzy Rule Base

T1–T6 respectively represent the capacitor switching, arc grounding, high frequency, fundamental, sub-frequency, single phase-to-ground, and T7 represents the line switching and lightning together.

Fuzzy rule base:

Rule 1: If $CQ1$ is A2 and $CQ2$ is B1 and $CQ3$ is C3 and $CQ4$ is D3 and $CQ5$ is E3 then T1 with $CF1$.

Rule 2: If $CQ1$ is A1 and $CQ3$ is C3 and $CQ4$ is D2 then T2 with $CF2$.

Rule 3: If $CQ1$ is A1 and $CQ3$ is C3 and $CQ4$ is D1 and $CQ5$ is E2 then T3 with $CF3$.

Rule 4: If $CQ1$ is A2 and $CQ2$ is B2 and $CQ3$ is C2 and $CQ4$ is D1 and $CQ5$ is E4 then T4 with $CF4$.

Rule 5: If $CQ1$ is A1 and $CQ3$ is C3 and $CQ4$ is D1 and $CQ5$ is E1 then T5 with $CF5$.

Rule 6: If $CQ1$ is A2 and $CQ2$ is B2 and $CQ3$ is C1 and $CQ4$ is D1 and $CQ5$ is E4 then T6 with $CF6$.

Rule 7: If $CQ1$ is A2 and $CQ2$ is B1 and $CQ3$ is C3 and $CQ4$ is D3 and $CQ5$ is E4 then T7 with $CF7$.

CF is the confidence factor or membership degree. Rule 1 as an example, $CF1$ is calculated by:

$$CF1 = \min \{ \mu_{A2} (CQ1), \mu_{B1} (CQ2), \mu_{C3} (CQ3), \mu_{D3} (CQ4), \mu_{E3} (CQ5) \}$$

For each characteristic quantity, seven confidences can be calculated through the fuzzy rule base. By locating the largest value, the type of over-voltage can be obtained. For the characteristic quantities in Table 1 as examples, the confidences for each one are obtained through fuzzy rules are listed in Table 4.

It can be seen from Table 4, the confidence factor is perfectly consistent with the type of over-voltage, (the maximum value is in the diagonal of the table). But the lightning over-voltage has high similarity with the line switching over-voltage. Therefore these two kinds of over-voltage should be classified by other approaches further.

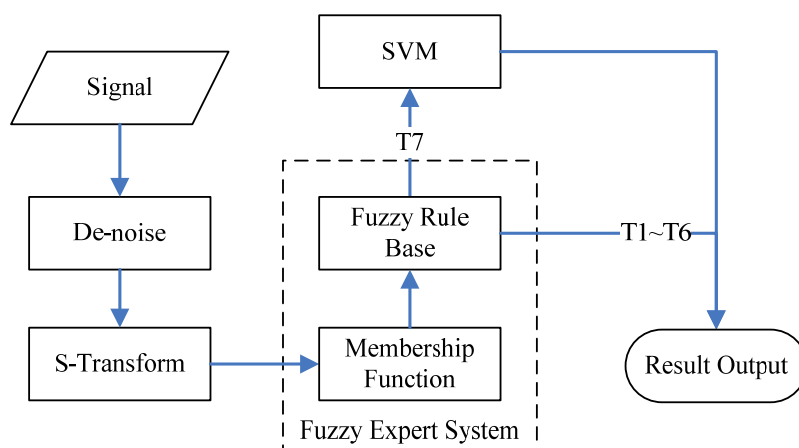
Table 4. Confidence factor of eight kinds of over-voltages.

Type	CF1	CF2	CF3	CF4	CF5	CF6	CF7
Capacitor switching	0.8985	0.0178	0	0	0	0	0
Arc grounding	0	0.7376	0	0.0074	0	0	0
High frequency ferroresonance	0	0.0172	1	0.0083	0	0	0
Fundamental ferroresonance	0	0.0214	0	0.9188	0.0111	0.0008	0.0001
Sub-frequency ferroresonance	0	0.0263	0	0.0012	0.9905	0	0.0111
Single phase-to-ground	0	0.0002	0	0.2535	0.0002	1	0
Line switching	0	0.0013	0	0	0	0	0.8706
Lightning	0	0.0124	0	0	0	0	0.8775

After the identification results obtained by the fuzzy expert system, if the result is line switching or lightning (T7), these two kinds of over-voltage need further identification procedures through *CQ6*. The second classifier in this procedure is SVM. SVM is proposed by Cortes and Vapnik in the 1990s [17]. SVM classifies two different data sets by finding the optimal hyperplane. In this system, through a large number of records training, the final employed SVM adopts the RBF kernel function and the width of the kernel function is 1.

5.4. Identification System Based on FES and SVM

The block diagram of the complete over-voltage identification system is drawn in Figure 10.

Figure 10. Block diagram of over-voltage identification system.

The advantage of this two step identification model is that, it can reduce the computational complexity effectively. The sampling rate of the original signal's head part is extremely high, which helps to distinguish the lightning and line switching over-voltage accurately through their high frequency oscillation. The identification of others does not need such a high sampling rate. Therefore this identification system will extract the feature from a high-resolution signal only when the type of over-voltage is T7 (lightning and line switching).

The de-noising method is chosen from the Kalman algorithm and the wavelet de-noise algorithm. For the wavelet de-noise algorithm, 45 kinds of mother wavelets from three wavelet families (Symlets, Daubechies, Coiflets), three kinds of threshold functions (soft, hard and compromise threshold),

four kinds of threshold selection rules (Stein's unbiased risk Estimate, heuristic SURE, universal and minimax threshold selection rule) were tested [18,19]. By comparing the de-noising effect of different methods for each kind of field over-voltage signal, the optimal de-noise scheme employed in this system is wavelet de-noise algorithm (six layer decomposition, sym12 mother wavelet, hard threshold and minimax threshold selection rule).

More than 300 field records from power substations were randomly selected from the database to verify the effect of the identification system. Limited by the length of the article, only parts of characteristic quantities and identification results are listed in this paper (Table 5).

Table 5. Characteristic quantities and identification results of 24 field over-voltages.

Type	Characteristic Quantities					Identification Results
	CQ1	CQ2	CQ3	CQ4	CQ5	
Capacitor switching	0.5951	1.0143	1.0101	33.9705	185	T1(Correct)
	0.5519	1.0415	1.0013	27.1107	190	T1(Correct)
	0.6330	1.1083	1.0194	45.2598	180	T1(Correct)
Arc grounding	0.2609	1.8658	0.4890	8.1343	145	T2(Correct)
	0.1856	1.8265	0.7340	7.0991	150	T2(Correct)
	0.3136	1.4472	0.9158	17.1156	20	T2(Correct)
High frequency ferroresonance	0.3608	2.9598	1.5899	2.2907	150	T3(Correct)
	0.3496	2.9571	1.6014	2.3197	150	T3(Correct)
	0.3370	2.9546	1.6147	2.3205	150	T3(Correct)
Fundamental ferroresonance	0.5990	1.7498	0.5775	3.1256	0	T4(Correct)
	0.6413	1.7021	0.5954	1.9397	0	T4(Correct)
	0.5265	1.6828	0.7097	7.0827	150	T2(Incorrect)
Sub-frequency ferroresonance	0.4020	1.0328	1.5833	2.1671	25	T5(Correct)
	0.4223	1.0977	1.5727	1.9389	25	T5(Correct)
	0.4233	1.1202	1.5081	2.3553	25	T5(Correct)
Single phase-to-ground	0.6200	1.7281	0.0126	2.4050	0	T6(Correct)
	0.6173	1.7276	0.2456	2.3049	0	T6(Correct)
	0.6181	1.7284	0.0126	2.3999	0	T6(Correct)
Line switching	0.5997	1.0096	0.9854	13.8765	10	T7(Correct)
	0.5845	1.0046	0.9786	20.8586	0	T7(Correct)
	0.6604	1.0152	1.0095	27.7779	0	T7(Correct)
Lightning	0.5533	1.0160	1.0235	17.5915	0	T7(Correct)
	0.6003	0.9902	0.9920	13.4594	0	T7(Correct)
	0.5756	0.9759	0.9792	18.1713	0	T7(Correct)

The final results for the entire samples are listed in Table 6.

Table 6. Final identification results.

Type	Rate (%)
Capacitor switching	95.0
Arc grounding	97.1
High frequency ferroresonance	100.0
Fundamental ferroresonance	97.0
Sub-frequency ferroresonance	100.0
Single phase-to-ground	100.0
Line switching	95.2
Lightning	97.9
Overall	97.8

6. Conclusions

In this paper a complete and effective smart over-voltage monitoring and identification system in which the monitoring system employs a new sensor installed at the tap of the transformer's bushing is presented. This sensor has the advantages of small size, high insulation levels and faster response. The installation of this system is easy and has no requirement for investment in primary equipment. The data acquisition mode can satisfy the high frequency sampling rate requirements for external over-voltage and long duration recording time requirements for internal over-voltage. The monitoring system and identification system are working independent of each other, and exchange the records by sharing the same database.

For the research of an over-voltage identification system, eight kinds of field over-voltage are discussed and analyzed in this paper. Aiming at the main feature of each kind of over-voltage, six well designed characteristic quantities are extracted through ST. FES and SVM are employed as classifiers. Based on a large amount of field data statistics, 14 membership functions and eight fuzzy rules are worked out. In order to reduce the computational complexity and improve the identification accuracy, the system is designed as a two step classification system, and SVM is used as the second classifier to distinguish the lightning and line switching over-voltage. This identification system is verified by more than 300 field records. The result shows that ST is suitable for over-voltage feature extraction and this identification system can identify and classify the over-voltage effectively and accurately.

Acknowledgements

This work was supported by the National Basic Research Program of China (973 Program) (2009CB724504) and the National 111 Project of China (B08036).

References

1. Juan, L.; Chenching, L.; Schneider, K.P. Controlled partitioning of a power network considering real and reactive power balance. *IEEE Trans. Smart Grid* **2010**, *1*, 261–269.
2. Pei, Z.; Fangxing, L.; Bhatt, N. Next-generation monitoring, analysis, and control for the future smart control center. *IEEE Trans. Smart Grid* **2010**, *1*, 186–192.

3. Mokryani, G.; Siano, P.; Piccolo, A. Identification of ferroresonance based on S-transform and support vector machine. *Simul. Model. Pract. Theory* **2010**, *18*, 1412–1424.
4. Mokryani, G.; Haghifam, M.R.; Esmailpoor, J. Identification of ferroresonance based on wavelet transform and artificial neural network. *Eur. Trans. Electr. Power* **2009**, *19*, 474–486.
5. Gu, Y.H.; Bollen, M.H.J. Time-frequency and time-scale domain analysis of voltage disturbances. *IEEE Trans. Power Deliv.* **2000**, *15*, 1279–1284.
6. Gaing, Z.L. Wavelet-based neural network for power disturbance recognition and classification. *IEEE Trans. Power Deliv.* **2004**, *19*, 1560–1568.
7. Kezunovic, M.; Yuan, L. A novel software implementation concept for power quality study. *IEEE Trans. Power Deliv.* **2002**, *17*, 544–549.
8. Stockwell, R.G.; Mansinha, L.; Lowe, R.P. Localization of the complex spectrum: the S Transform. *IEEE Trans. Signal Process* **1996**, *44*, 998–1001.
9. Fengzhan, Z.; Rengang, Y. Power-quality disturbance recognition using s-transform. *IEEE Trans. Power Deliv.* **2007**, *22*, 944–950.
10. Dash, P.K.; Panigrahi, B.K.; Panda, G. Power quality analysis using s-transform. *IEEE Trans. Power Deliv.* **2003**, *18*, 406–411.
11. Mishra, S.; Bhende, C.N.; Panigrahi, B.K. Detection and classification of power quality disturbances using s-transform and probabilistic neural network. *IEEE Trans. Power Deliv.* **2008**, *23*, 280–287.
12. Àkànbí, L.A.; Odéjobí, O.À. Automatic recognition of oral vowels in tone language: Experiments with fuzzy logic and neural network models. *Appl. Soft Comput.* **2011**, *11*, 1467–1480.
13. Liao, Y.; Lee, J.B. A fuzzy-expert system for classifying power quality disturbances. *Int. J. Electr. Power* **2004**, *26*, 199–205.
14. Monsef, H.; Ranjbar, A.M.; Jadid, S. Fuzzy rule-based expert system for power system fault diagnosis. *IEE Proc. Generat. Transm. Distrib.* **1997**, *144*, 186–192.
15. Yen, V.C. Rule selections in fuzzy expert systems. *Expert Syst. Appl.* **1999**, *16*, 79–84.
16. Zadeh, L.A. Fuzzy sets. *Inf. Control* **1965**, *8*, 338–353.
17. Cortes, C.; Vapnik, V. Support-vector networks. *Mach. Learn.* **1995**, *20*, 273–297.
18. Donoho, D.L. De-noising by soft-thresholding. *IEEE Trans. Inf. Theory* **1995**, *41*, 613–627.
19. Hao, Z.; Blackburn, T.R.; Phung, B.T.; Sen, D. A novel wavelet transform technique for on-line partial discharge measurements. Part 1: WT de-noising algorithm. *IEEE Trans. Dielectr. Electr. Insul.* **2007**, *14*, 3–14.